Hydro-elastic coupling effect on the dynamic global response of a spar-type floating offshore wind turbine

Cesar. Aguilera [1], **Romain. Ribault** [2], **Jerome. De-Lauzon** [3], **and Adrien. Hirvoas** [2]

[1]Sercel, 16 Rue du Bel air, 44470 Carquefou, France
[2]France energies Marines, 525 Av. Alexis de Rochon, 29280 Plouzané, France
[3]Bureau Veritas, 1 place Zaha Hadid, 92400 Courbevoie, France

Correspondence: Cesar. Aguilera (cesar.aguilera@sercel.com)

Abstract. Designing floating wind turbine systems requires integrated load assessments (ILA) using fully coupled hydro-servo-aero-elastic models. ~~While~~ In most cases, floater hydrodynamics are represented using potential flow models ~~are commonly used to represent floater hydrodynamics~~ for mooring system design and motion estimation, ~~the floater is tipically assumed as~~ while the floater itself is typically assumed to behave as a rigid body. ~~This~~ However, this assumption can significantly ~~impact~~ affect tower eigenfrequency calculations, ~~particularly~~ especially for large floaters. In this study, we investigate these effects using in-situ sensor data from the Zefyros 2.3 MW spar wind turbine. We ~~detail the methodology employed~~ present a methodology to accurately determine tower's eigenfrequencies. A rigid floater model without added mass ~~resulted in a 37% error~~ leads to an average error of 38% compared to measured ~~modes. Incorporating floater flexibility and added mass reduced this error to~~ tower modes. Including hydrostatic added mass reduces the error to 28%. Further incorporating floater flexibility decreases the error to 5%, and ~~further to~~ accounting for blade flexibility lowers it to just 3%~~with blade flexibility~~ . These discrepancies highlight the ~~necessity~~ importance of refining the hydro-servo-aero-elastic model to ~~match the~~ align with eigenfrequencies derived from finite element hydro-structural analyses. We present potential model adjustments~~and discuss their impacts. After implementing one model modification, we present the results and illustrate the updated model~~ , assess their impacts, and demonstrate the updated validation process. ~~-~~

1 Introduction

Offshore wind energy has ~~grown rapidly~~ experienced rapid growth over the past decade, with ~~a threefold increase in capacity~~ capacity tripling between 2012 and 2022. During this period, ~~a significant average annual wind capacity~~ an average of ~~55GW was added ; and 75GW only~~ 55 GW of new wind capacity was added annually, reaching as much as 75 GW in 2022 alone (IRENA , 2023). According to ~~the~~ IRENA (2023)'s 1.5°scenario~~(IRENA , 2023)~~, wind energy ~~will be~~ is expected to become one of the largest sources of electricity worldwide~~with a prediction of~~ , with an estimated 10,300 GW of installed capacity by 2050.

~~At the same time, the development of wind energy faces the problem of having a~~ Despite this expansion, the sector continues to face the challenge of a relatively high levelized cost of energy (LCOE) compared to other ~~sectors. Given the collaborative researchefforts during the design and development,~~ power generation sources. However, collaborative research, supportive government policies, and ~~the significant increase in asset production in recent years, the domain has considerably~~ advances in large-scale asset production have significantly reduced the LCOE of Floating Offshore Wind Turbines (~~FOWT)making them more~~ FOWTs), making them increasingly cost-competitive (WindEurope , 2020).

One strategy for ~~the~~ cost reduction is to increase the ~~individual asset power generation, which increases at the same time the general~~ power output of individual turbines. This approach, however, also requires a proportional increase in the overall structural size. As ~~the floater structure also increases in size, this leads to a design of more flexible support structures~~floating foundations scale up, they must be designed to remain stable and flexible under more demanding conditions.

The design of ~~the support structure~~ support structures for FOWTs is ~~not an easy task. This is mainly~~ particularly challenging due to the complex ~~phenomena that must be considered as these assets are deployed in very hostile environments (European Commission , 2019). Thus~~physical phenomena involved and the harsh marine environments in which they operate (European Commission , 2019). Consequently, the continuous ~~evolution of the design of larger structures is now a concern in the~~ trend toward larger and more powerful turbines raises new concerns for the engineering and design community.

Currently, only a few FOWTs are operational. Zefyros (shown in figure 1), is one them. This wind turbine is located 11 km far from the coast of Norway and ~~now~~ owned by Unitech. It is the first multi-megawatt floating turbine in the world (Skaare et al. , 2014). The first numerical model of Zefyros was presented in the work of Skaare et al. (2007). In this work, the structure was modeled using a coupled simulation based on two different software's, SIMO/RIFLEX and HywindSim, developed by Marintek and Risø National Laboratory respectively. Both simulators solve their own dynamic equilibrium equations in time domain. A scaled set of tests cases were carried out by Ocean Basin Laboratory at Marintek with the objective to compare the results of an integrated coupled simulation tool outputs with experimental data. A good agreement was shown between simulation and measurement data.

Many studies ~~using~~ employing aero-hydro-servo-elastic simulations of FOWTs (e.g., (C.P.M. Curfs , 2015; Cheng et al. , 2015; Zhang et al. , 2020)) ~~consider~~ account for tower and blade flexibility. However, when ~~focusing~~ the focus is on mooring design or ~~FOWT motion, potential flow models are often used for floater hydrodynamics . Although these models accurately~~ platform motion, floater hydrodynamics are often modeled using potential flow theory. While these models capture hydrodynamic loading ~~, they typically assume a rigid floater . This rigidity~~ with reasonable accuracy, they generally assume the floater to be rigid. This assumption not only precludes ~~calculating internal floater loads but also impacts tower eigenfrequency calculations, potentially affecting tower~~the estimation of internal loads within the floater but also influences the calculation of tower eigenfrequencies, which in turn may affect predictions of the tower's dynamic response.

~~The effect of the floater flexibility on the~~

The importance of considering floater flexibility in global dynamic responses ~~of a 15MW~~ has been emphasized in recent studies. For example, Li et al. (2023) investigated a 15 MW semi-submersible ~~floating wind turbinehas been highlighted in the work of Li et al. (2023). Zhixin et al. (2022) have proposed a method to include flexibility of~~ wind turbine, highlighting the influence of structural flexibility on its dynamic behavior. Similarly, Borg, Michael and Hansen, Anders Melchior and Bredmose, Henrik (20 proposed an approach to incorporate large-volume ~~substructures based on an iterative procedure between~~ substructure flexibility using an iterative coupling between the radiation-diffraction solver WAMIT and the aeroelastic code HAWC2 ~~software's~~ for a spar-type ~~substructure. In this work, a dynamic comparison of the global response between~~ platform. Their study compared the global responses of rigid and flexible ~~model was performed~~models, showing that ~~flexibility provides additional information to derive~~ accounting for flexibility yields more accurate sectional ~~loads~~load predictions.

As ~~it has been shown , this flexibility effect is addressed~~ shown in the literature~~for different floating support structure types~~ , the effect of floater flexibility has been addressed for different types of floating support structures and wind turbine sizes. ~~In~~ According to DNV-RP-0286 (DNV-GL , 2019)~~it is mentioned that this hypothesis may be sufficient~~ , the assumption of rigid-body behavior may be acceptable in certain cases, ~~and before implementation, it should~~ provided it

Figure 1. Zefyros, the world's first multi-megawatt FOWT UNITECH (2022). Credits: Unitech Energy Group

Figure 2. ~~Zefyros,~~ Sensor position along the ~~world's first multi-megawatt FOWT UNITECH (2022)~~tower.~~Credits: Unitech Energy Group~~

can be demonstrated that ~~the flexibility of the floating device does not have a significant influence on the response of the turbine.~~ floater flexibility does not significantly influence the turbine's response. Similarly, NR572 (Bureau Veritas , 2015) ~~also mention~~ states that hydro-elasticity ~~needs to be considered where appropriate~~should be considered when relevant. However, ~~today there is no clear guidance on the recommended practices for~~ despite these references, there is currently no clear or unified guidance on best practices for assessing the validity and ~~application of the substructure rigid body~~ applicability of the rigid-body simplification during the design phase of floating substructures.

This article details a methodology to accurately calculate tower eigen-frequencies at design stage and integrate floater flexibility effect into the aero-hydro-servo-elastic simulations. We demonstrate the impacts of floater rigid body assumption on tower eigenfrequency calculation, using in-situ sensor data from the Zefyros 2.3 MW spar wind turbine. Section ~~2~~ 1.1 briefly introduces the Zefyros wind turbine. In Section ~~??~~2.1, we describe the measurement campaign and the estimation of tower eigenfrequencies, among other dynamic parameters, using the S-Morpho measurement system. In Section ~~??~~2.2, we describe the numerical models. The subsection ~~??~~ 2.2.1 provides some theoretical background on the hydro-structural model used for modal analysis and reference calculation of the tower eigenfrequencies. Then, in Section ~~??~~2.2.2, we describe the initial aero-hydro-servo-elastic simulation model implemented in OpenFAST. In Section ~~??~~2.2.3, is presented the potential simulation model adjustments, discussing their limitations and impacts. For the tower's eigenfrequency calculation from time-domain simulation results, we used an Operational Modal Analysis (OMA) ~~tool~~ described in Section ~~??~~2.2.4. In section ~~??~~ 3 we describe the load cases we used to run the aero-hydro-servo-elastic models in order to assess tower eigenfrequency in time domain simulation and identify a potential modification of the global dynamic tower response . Section 4 is dedicated to the discussion and the presentation of the results.

1.1 Description of Zefyros floating wind turbine

Unitech Zefyros is a floating spar offshore wind turbine originally installed as Hywind Demo by Equinor (Statoil) at approximately 11 kilometres of the west cost of Karmøy (Norway). The floater is based on a cylinder shape submerged vertically and connected to a steel tower. Having a spar-type substructure, the structure is stabilized due to the long distance between the center of gravity and center of buoyancy. This system is supporting a Siemens 2.3 ~~MW~~ MW wind turbine with a rotor diameter of 82.4 meters.
The system is fixed to the seabed by three mooring lines con-

Table 1. Wind turbine characteristics.

Parameter	Value/Unit
Turbine power	2.3 MW
Turbine weight	138 tons
Draft hull	100 m
Nacelle height	65 m
Rotor diameter	82.4 m
Water depth	220 m
Mooring	3 lines
Diameter at water line	6 m
Diam. submerged body	8.3 m
Rotor speed	6 – 18 rpm
Wind speed range	3 – 25 m/s

sisting of hybrids wires and clump weights. The length of each line is approximately 800 metres.The hull is ballasted with gravel and water. The main particulars of Zefyros are given in Table 1. For a detailed description of the structure refer to the work of Sjur Neuenkirchen Godø (2013).

~~Wind turbine characteristics.Parameter Value/UnitTurbine power 2.3 MW Turbine weight 138 tons Draft hull 100 mNacelle height 65 mRotor diameter 82.4 mWater depth 220 mMooring 3 linesDiameter at water line 6 mDiam. submerged body 8,3 mRotor speed 6 – 18 rpmWind speed range 3 – 25 m/s~~

2 Methodology

2.1 Measurements performed on 2.3MW Zefyros wind turbines

Dynamic and static measurement data ~~was collected continuously during two years . This acquisition was done in~~ were collected continuously over two years within the framework of the DIONYSOS project using the S-Morpho system. ~~Outputs of the sensor system include ,~~ The sensor outputs include three-axis accelerations, magnetic field, and temperature at a sampling frequency of $40Hz$. Six sensors were installed along the Zefyros tower in May 2022, approximately 30° west-north.

~~The sensors were positioned~~ Their positions were at 17, 33, 41, 49, 57, and 63 ~~meters~~ m above sea level. The local sensor reference frame was ~~fixed to the towerreference frame, and the *X* and *Y* direction corresponds to the~~ aligned with the tower's reference frame: the X-axis corresponds to fore-aft ~~and~~ movement, the Y-axis to side-to-side movement~~respectively~~, and the ~~*Z* as vertical movements~~Z-axis to vertical movement.

~~On figure 2 are shown~~ Figure 2 shows the first two sensors installed on the tower. As the tower is made of steel, all sensors were fixed by two powerful magnets per unit. A general view of the positioning is ~~depicted on figure 4. For more~~ provided in figure 3. For further details about the sensor system~~please refer to (Redoute, T. , 2020)~~, refer to Redoute, T. (2020).

~~Sensor position along the tower.~~

2.1.1 Modal Identification of Zefyros Tower From Measurements

The simulation of the dynamic behavior of a wind turbine is ~~strongly~~ highly dependent on the accuracy of ~~the~~ its numerical model. ~~Therefore, calibration of the model is required based on reliable experimental data to correctly reproduce~~ To ensure the model correctly reproduces the dynamic response of the asset~~. The experimental selected data for this~~ , calibration must be performed using reliable experimental data. In this work, the selected experimental data for calibration were the global modal parameters.

The Zefyros wind turbine is equipped with a yaw system~~that allows the rotation of the nacelle to keep it facing~~ , which allows the nacelle to rotate and remain oriented toward the wind direction. This ~~property makes~~ feature adds complexity to the modal analysis~~more complex for wind turbines~~, as the ~~modal deformation of the structure is dependent~~ structural modal deformations depend on the nacelle orientation (Oliveira et al. , 2018). To ~~overcome the problem of the nacelle~~ address the challenge of combining the moving reference frame ~~and the tower~~ of the nacelle with the fixed reference frame ~~, the following~~ of the tower, a coordinate transformation was ~~performed using~~ applied. The transformation used the nacelle orientation angle, obtained from the SCADA data ~~,~~ provided by Unitech Energy Group.:

$$\begin{bmatrix} x'(t,\theta) \\ y'(t,\theta) \\ z'(t,\theta) \end{bmatrix} = R(\theta) \cdot \begin{bmatrix} x(\theta) \\ y(\theta) \\ z(\theta) \end{bmatrix} \quad (1)$$

Where the variables x and y contain the raw acceleration data, variables x' and y' are the new transformed accelerations and corresponds to the yaw angle θ of a 10 min averaged. $R(\theta)$ is the three axes matrix rotation.

~~The mentioned coordinate transformation made possible to represent the acceleration signal of the sensors and project them~~ This coordinate transformation enables the projection of the measured acceleration signals into the fore-aft and side-to-side directions of the ~~turbine, horizontal orthogonal to the rotor plane and horizontal parallel direction~~ wind turbine — i.e., the directions parallel and perpendicular to the rotor plane~~respectively.~~, respectively. The transformation was applied to the entire dataset collected during December 2022, allowing comparison with SCADA data acquired for the same period.

After ~~preprocessing, the~~ performing the transformation, reference modal parameters were estimated from a 20-minute interval when the wind turbine operated under rated conditions. The environmental parameters corresponding to this operating condition are summarized in

table 3.
Subsequently, the transformed acceleration data ~~is processed in a continuous manner using OMA~~ were continuously processed for the entire month using Operational Modal Analysis (OMA) techniques for wind turbine structures when external excitation cannot be measured (van Vondelen et al. , 2022). ~~As example, in figure 3 is shown the modal tracking~~ In order to estimate and track the modal frequencies and mode shapes over time, the covariance-driven Stochastic Subspace Identification (SSI-COV) method was employed (Masjedian, M.H. and Keshmiri, Mehdi , 2009),using six reference channels and a time lag of 10 seconds. The analysis provided parametric estimations within 20-minute moving windows. To ensure the correct modal shape tracking over time, the Modal assurance criterion (MAC) was used to assess the correlation between the continuously estimated and reference mode shapes (Pastor et al. , 2012). When the MAC value exceeded 0.9, the corresponding mode shape was retained as a valid tracked mode.
Figure 4 illustrates the temporal evolution of the second fore-aft and side-to-side tower modes during December 2022~~as~~ , shown by the pink and red lines, respectively. The black line ~~depicts the time series of the rotor rotation in RPM~~represents the rotor rotational speed in RPM, derived from SCADA data. This ~~image shows the effect that has the~~ figure highlights the influence of rotor rotation on the tower's modal frequencies. ~~The modal analysis algorithm used for the study is the so-called covariance-driven stochastic subspace identification (SSI-COV) method with 6 reference channels and for 20 minutes time windows. For more detail of the method, please refer to (Masjedian, M.H. and Keshmiri, Mehdi , 2009). The~~ The emerged frequencies of the structure are shown in table 4. A more detailed description about the ~~calculation~~ computational methodology can be found in the document of SERCEL (2024).

2.2 Numerical models

In the following subsections~~the methodology calculation on each software~~ , the calculation methodology for each software tool is briefly described. It ~~must be mentioned that Homer has been used~~ should be noted that Homer was employed as the offshore modal analysis tool, solving the classic equation of motion (equation 3). ~~Regarding the~~ For coupled dynamic time-domain simulations ~~for wind turbines~~of the wind turbine, an OpenFAST model was developed and tested. A summary of the two numerical model characteristics is given in table 2. A more detailed description is given in the following sections.

Figure 3. ~~Plot~~ Graphic representation of the ~~second tower natural frequency tracking correlated with the rotor rotation during December 2022~~finite element model used in Homer software

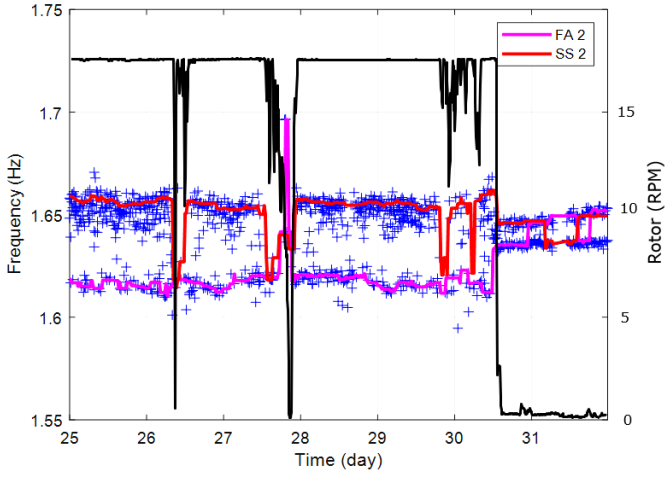

Figure 4. ~~Model main characteristics in function~~ Plot of the ~~numerical software.~~second tower natural frequency tracking correlated with the rotor rotation during December 2022
~~software Flexible floater Rigid nacelle Flexible bladesHomer x/OpenFAST x~~

2.2.1 Hydro-Structure Model To Perform Tower's Eigenfrequency Reference Calculation

To calculate the reference eigenfrequencies of the tower, the analysis was carried-out in Homer, an Hydro-structure software with modal analysis capability developed by Bureau Veritas (Malenica et al. , 2013). The model implemented in Homer describes the full mechanical FOWT system and is derived from an ANSYS model (figure ~~4). In this analysis, the~~ 3). The floater and tower are ~~all discretized~~ build with shell elements. Rotor Nacelle Assembly is modelled as a mass element, connected to the tower ~~with a rigid element~~rigidly. Blades are also modelled, either as flexible beam elements, or by just considering their inertia.

The hydro-elastic analysis performed in Homer relies on the decomposition of the structural response of the floating wind turbine on its N first dry vibration modes. Instead of solving a 6-by-6 linear problem, the dimension of all matrices (mass, added mass, stiffness) is increased to $6+N$.

The first step in the coupled analysis is therefore a dry modal analysis of the structure. When the flexible modes have been chosen, the hydrostatic stiffness is computed for the N vibration modes, as well as for the six rigid body motions (surge, sway, heave, roll, pitch, and yaw). The hydrodynamic radiation boundary value problem is then solved by Hydrostar for the $6+N$ modes, and the added mass matrix is then assembled. Finally, the wet eigen-modes and frequencies are computed. The method is rather well known and has been the subject of many scientific publications (Malenica et al. , 2008). The pre-stressing at hydrostatic equilibrium is not considered in this analysis; its influence is assumed to be small.

Bureau Veritas Hydrostar software is used to solve the radiation boundary value problems for the rigid body motions, as well as for the vibration modes. For each vibration mode, the additional body boundary condition becomes:

$$\frac{\partial \varphi_{Rj}}{\partial n} = \mathbf{h^j} \cdot \mathbf{n} \tag{2}$$

~~Graphic representation of the finite element model used in Homer~~

Where φ_{Rj} is the radiated velocity potential for mode j and $\mathbf{h^j}$ is the shape of mode j, interpolated from the finite element model to the hydrodynamic mesh. Once all radiation boundary value problems (6 rigid motions and N elastic modes) have been solved, the radiation pressures are computed at the center of the finite elements, and integrated to compute the added masses. The motion equation can then be written as (after removing the excitation forces and radiation damping):

$$(-\omega^2[M+A(\omega)]+[K+C])\{\xi\}=0 \tag{3}$$

Table 2. Model main characteristics in function of the numerical software.

software	Flexible floater	Rigid nacelle	Flexible blades
Homer	✓	✓	x/✓
OpenFAST	x	✓	✓

With $[K]$ the structural stiffness, $[C]$ the hydrostatic stiffness, $[M]$ the structural mass, $[A(\omega)]$ the added mass and $\{\xi\}$ the vector of modal amplitudes.

For each frequency ω, the inverse of the total mass (including added mass) is computed and multiplied by the total stiffness. The resulting matrix is finally diagonalized for each frequency to find the wet eigen-frequencies and eigen-vectors. For each eigen-mode computed by the diagonalisation, the vibration frequency is obtained when the eigen-frequency matches the frequency used for the added mass.

$$[M+A(\omega)]^{-1}[K+C]\{\xi\}=\omega^2\{\xi\} \tag{4}$$

2.2.2 ~~Initial Aero-Hydro-Servo-Elastic Simulation Model~~

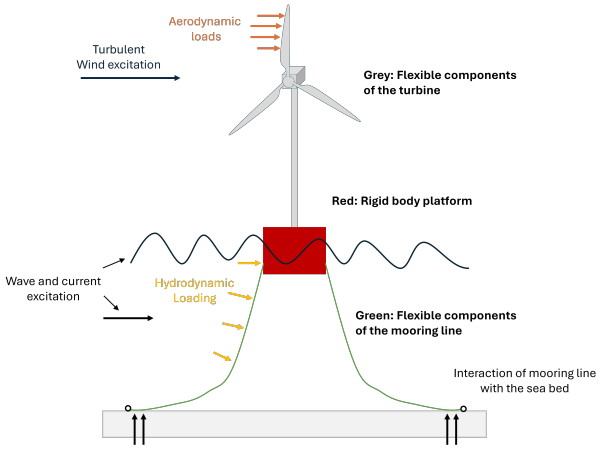

Figure 5. Schematic overview of the FOWT modeling approach in OpenFAST.

2.2.2 Initial Aero-Hydro-Servo-Elastic Simulation Model

OpenFAST (FAST stands for Fatigue, Aerodynamics, Structures, and Turbulence) is an open-source engineering code distributed by the National Wind Technology Center (NWTC) (Jonkman et al. , 2005). This code is a nonlinear time-domain simulator that employs a combined modal and multibody structural-dynamics formulation. In our research, the numerical representation of the Zefyros system has been implemented within OpenFAST. This model assumes a rigid platform but accounts for the tower's flexibility, see Figure 5. The structural, hydrodynamic, and aerodynamic properties of

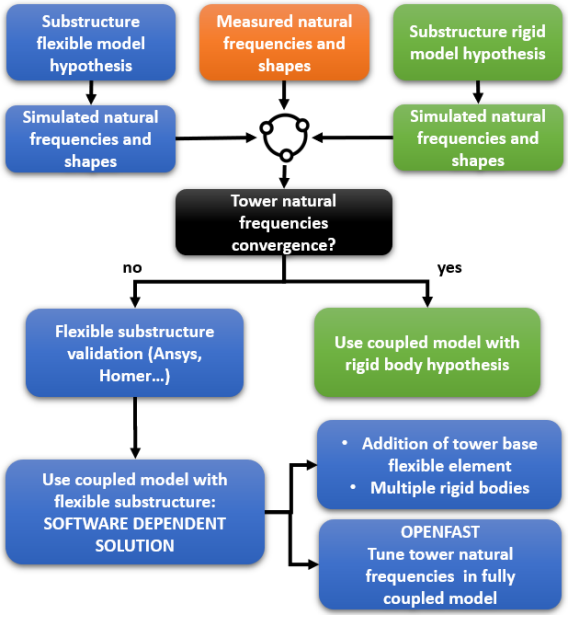

Figure 6. Schematization of the methodology followed in this study.

the FOWT were configured based on publicly available documents and generic wind turbine data interpolation. The key properties defined include inertial characteristics of the nacelle, lift and drag profiles of the airfoil, along with mass and structural-elastic properties at various blade locations, inertial and structural-elastic characteristics of the drive train, mass and structural-elastic properties at specific tower locations, from the waterline to the tower's top, and inertial properties of the rigid spar.

To prevent drifting, the Zefyros platform is anchored to the seabed using three separate catenary mooring lines attached to anchors at the seafloor. For the numerical representation of mooring line dynamics, we used MoorDyn, a dynamic lumped mass model within OpenFAST (Hall , 2015). This numerical modeling methodology leverages this model's capability to represent multi-segmented mooring lines, comprising diverse elements such as chains, unsheathed spiral ropes, and additional clump weights, as outlined in Hirvoas (2022). The latest version of MoorDyn enables modeling two-leg bridles, significantly improving the yaw natural period from previous versions (Hall , 2020).

Incorporating hydrodynamics into the numerical simulation requires accurately defining incident wave characteristics and hydrodynamic loading representations (Molin, Bernard , 2023). Within this OpenFast framework, HydroDyn is the module designed to calculate these hydrodynamic loads in the time domain (Jonkman, Jason M and Robertson, AN and Hayman, Greg J , 2014). To obtain the hydrodynamic loads acting on the rigid body platform, a pre-computation step using radiation-diffraction software with a second-order loading module is necessary to solve different hydrodynamic theories. Finally, in our full-scale study, we calibrated the mooring radius and the platform's displaced volume to match the system's natural periods with low relative errors, as evaluated using in-situ data.

~~Schematic overview of the FOWT modeling approach in OpenFAST.~~

Additionally, we adapted the ROSCO NREL controller, as described in ~~(Abbas et al. , 2022)~~Abbas et al. (2022), to the simulation model and conducted different dynamic load cases, comparing them with field measurements. The results show that the floating platform movements closely match the measured data, indicating good agreement as shown in Hirvoas (2022).

2.2.3 Possible aero-hydro-servo-elastic model modification and impacts

When ~~it~~ modification of the aero-hydro-servo-elastic model is required to ~~modify the model aero-hydro-servo-elastic to match the simulation model's tower eigen-frequencies~~ align the simulated tower eigenfrequencies with the measured ~~/ calculated one~~or calculated values, several approaches can be ~~used. The first option to investigate is to make the floater~~ applied. A first option is to model the floater as a flexible body, using a ~~beam element discretisation and distribute~~ beam-element discretization and distributing the hydrodynamic loading ~~calculations over each beam~~ over each element. This ~~will provide access to~~ provides access to the internal loads of the floater ~~,~~ at the chosen ~~discretisation~~ discretization scale. Two types of hydrodynamic models can be ~~used~~ employed :

1. Distributed potential flow hydrodynamic model.
2. Distributed Morison elements.

Thomsen et al. (2021) and Xu et al. (2019), ~~used~~ applied a full Morison approach for the hydrodynamic model and beam elements for mechanical model of the floater. Such approach can lead to satisfactory FOWT global model with floater flexible models. However, Morison hydrodynamics model has its own limitations (Leroy et al. , 2021) and coefficients are not available for all floater shapes which makes the approach not applicable for some floater designs (Guignier, Lucie and Courbois, Adrien and Mariani, Riccardo and Choisnet, Thomas , 2016).

To ~~model the floater hydrodynamics with potential theory while modeling the floater as a flexible body~~overcome these constraints, several initiatives ~~explored equivalent approaches . They combine~~ have investigated equivalent approaches that combine potential-flow theory with flexible floater modeling. These methods leverage the multi-body or additional generalized modes capabilities of radiation–diffraction software (~~Wamit, Hydrostar, Diodore, etc…) with beam element models of~~ e.g., WAMIT,

HydroStar, Diodore) in combination with beam-element aero-hydro-servo-elastic ~~software (such as Orcaflex, Deeplines or SIMA)~~solvers (e.g., OrcaFlex, Deeplines, SIMA). In such frameworks:

- The radiation diffraction software calculates several hydrodynamic database (HDB) on a floater discretisation equivalent to the mechanical model discretization.
- The floater is mechanically modeled as an assembly of beam elements in aero-hydro-servo-elastic software and for each beam element, the corresponding HDB is associated.

This type of approach was applied to the Ideol's floater, using Ansys Aqwa as the radiation diffraction software and Orcaflex as the aero-hydro-servo-elastic software (Guignier, Lucie and Courbois, Adrien and Mariani, Riccardo and Choisnet, Thomas , 2016); ~~They used~~ In their work, a multibody approach ~~for the radiation-diffraction calculations with Aqwa. They discretized the floater in several compartmentsand calculated HDs~~ was implemented in Aqwa, where the floater was discretized into several compartments. HDBs were then computed, including the hydrodynamic interactions between compartments. However, ~~they needed to artificially separate the compartments in Aqwa code to avoid~~ to prevent divergence of the calculations, the compartments had to be artificially separated within the Aqwa code.

A similar but different approach was applied to a spar platform, supporting the DTU 10 MW by Xiaoming et al. (2023); and a three-column semi-submersible floaters by Chenyu et al. (2017) and by Li et al. (2023). They all used Wamit as a Radiation-Diffraction software and an in-house code to integrate panel pressure per floater sub-structure to compute the added mass, damping and excitation forces with a discretization adapted to the mechanical model of the floater.

In the above cited approaches, hydrodynamic interactions between sub-structures are taken into account, but the hydrostatic/hydrodynamic loads are not influenced back by floater flexibility. Chenyu et al. (2017) acknowledged that the influence of the inertia loads and hydro loads induced by the flexible modes of the hull shall be investigated in future. To account for deformable modes of a floater contribution into hydrodynamic loads, within a small deformation assumption, Borg, Michael and Hansen, Anders Melchior and Bredmose, Henrik (2016) proposed an iterative procedure between aero-hydro-servo-elastic (HAWC2) and WAMIT. Additional generalized modes calculation option may also be used de Lauzon Jérome (2024) and are available in Homer software. Xiaoming et al. (2023) performed an experimental validation such an hydro-structural coupled model, demonstrating that internal floater loading estimations where more accurate with a distributed potential flow hydrodynamic model rather than with a Morison hydrodynamic model.

When the above approaches cannot be implemented, other options are available :

1. Prolongate the tower mechanical model with a virtual element inside the floater and calibrate the mechanical properties to match the tower eigenfrequencies.
2. Modify the global stiffness modal parameter in OpenFast, such an option is available inside the Elastodyn file

In our case, the ~~only feasible~~ chosen option was to modify the global tower stiffness. ~~Indeed our OpenFAST model~~ The OpenFAST model employed did not include the ~~Subdyn modulewhich would allow the tower~~ SubDyn module, which would have enabled the representation of the tower's prolongation below the floater~~/~~–tower interface. ~~Because the eigenfrequency mismatch was quite significant in our case~~Given the significant mismatch in eigenfrequencies, adding a small structural element at the ~~bottom of the tower was not a workable~~ tower base was not considered a viable option. It ~~shall be noted that Hydrodyn and Subdyn modules were recently updated with the capabilities to model~~ is worth noting, however, that recent updates to the HydroDyn and SubDyn modules now include capabilities for modeling flexible floaters.

2.2.4 Verification tool of simulated tower frequencies and shapes

To ~~check~~ verify the tower eigenfrequencies ~~of~~ from the aero-hydro-servo-elastic ~~model against~~ setup against those obtained from the hydro-structure calculation model, ~~it is required to perform~~ a modal analysis ~~on the aero-hydro-servo-elastic model. The aero-hydro-servo-elastic model are used to run time domain simulations~~is required. This comprehensive model is primarily used for time-domain simulations, where most of the physics ~~in the wind turbine modeling~~ are nonlinear. ~~A~~ Consequently, a specific linearization of ~~a specific~~ the state-space ~~is required~~ representation is necessary to perform eigenanalysis. Most ~~of the softwares have such modal analysis module included. In our OpenFast model~~software tools include built-in modules for this purpose. Here, two options were available:

~~Schematization of the methodology followed in this study.~~

- the use of the linearization functionality included in the OpenFAST open-source code
- running OMA techniques on the OpenFAST output acceleration data.

Even thought the OpenFAST funcionality has been widely used and verified for FOWTs as demonstrated in ~~(Johnson et al. , 2019)~~Johnson et al. (2019), in this study the validation of the natural frequencies and shapes was estimated via OMA already used when estimating the modal parameters of measured data, described in section ~~??.~~ 2.1.1.

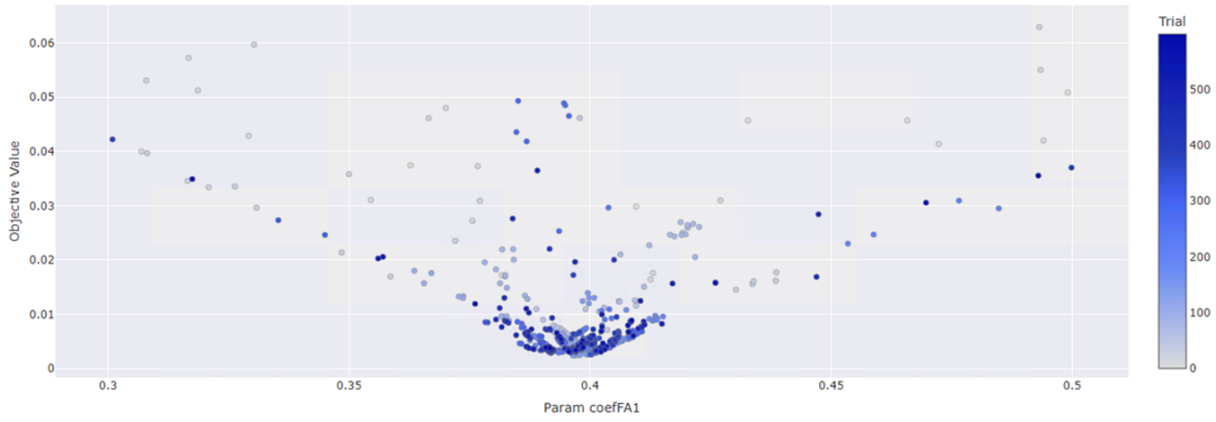

Figure 7.

2.3 Load cases for evaluation of dynamic tower response in time domain calculations

The first stage ~~on~~ of the proposed methodology consisted of determining the sensitivity of the tower modes to the floater rigidity. In the second stage, the aero-servo-hydro-elastic model ~~is adapted to take into account the flexibility of the floater. To do that~~was adapted to account for the floater's flexibility. To achieve this, two main load cases were analyzed in order to investigate the global ~~response of the structure, in a low and rated condition. The criteria for low wind load conditionwas that wind should be lower than $12m/s$ with a~~ structural response under both low-wind and rated conditions.

- Low wind condition: wind speed below 12 m/s and significant wave height ~~smaller than $2m$. For rated condition, the wind speed and wave height should have values around $13m/s$ and $3.5m$ respectively. In table 3 are described the~~ below 2 m.
- Rated condition: wind speed around 13 m/s and significant wave height of approximately 3.5 m.

The full set of input parameters ~~of the~~ for these two load cases ~~. The time series of~~ is presented in table 3. The irregular wave elevation ~~were modeled with~~ time series were modeled using a JONSWAP spectrum~~. The~~ , while the time-varying wind loads were ~~calculated using Turbsim~~generated with TurbSim, a full-field ~~turbulent-wind~~ turbulent wind simulator (Jonkman , 2016).

2.4 Parametric optimization

Once the load cases and the parameters to be optimized were defined, a parametric study was carried out to optimise the global stiffness modal parameter in OpenFAST, available inside the Elastodyn module. This was achieved by the open-access Python package SimuOptuna (Ribault, Romain. , 2024). The package is based on the Optuna hyperparameter optimization framework (Akiba et al. , 2019), specifically adapted for wind turbine simulation tools. The configuration of the optimization routine was as follows:

- Sampler: tree-structured parzen sampler (TPS)
- number of trials: 600
- Loss function : Mean squared error between measured and simulated natural frequencies. Natural frequency identification methodology is described in section 2.1.1.

Since the tower factors vary between 0 and 1, these limits were used to constrain the objective function. Figure 7 illustrates the parametric space and sampling iterative evolution of the first fore-aft tower factor. The color bar indicates the sequential iterations, showing how the objective function value decreases over time. The adjustment factor for the first side-to-side mode was estimated using the same procedure. The optimized values obtained for the first tower modes were 0.397 (fore-aft) and 0.421 (side-to-side). For more details on the parameter optimization process, refer to Ribault, Romain. (2024).

Table 3. Load cases characteristics of 1 hour average values. Low condition of 02/12/2022 at 3 p.m. And Rated condition of 06/12/2022 at 10 p.m.

Load case	Low condition	Rated condition
Wave height [m]	1.36	3.3
Wave direction [°]	273	336
Wave period [s]	13	8
Wind speed [m/s]	1.92	15.1
Wind direction [°]	70.88	354.7

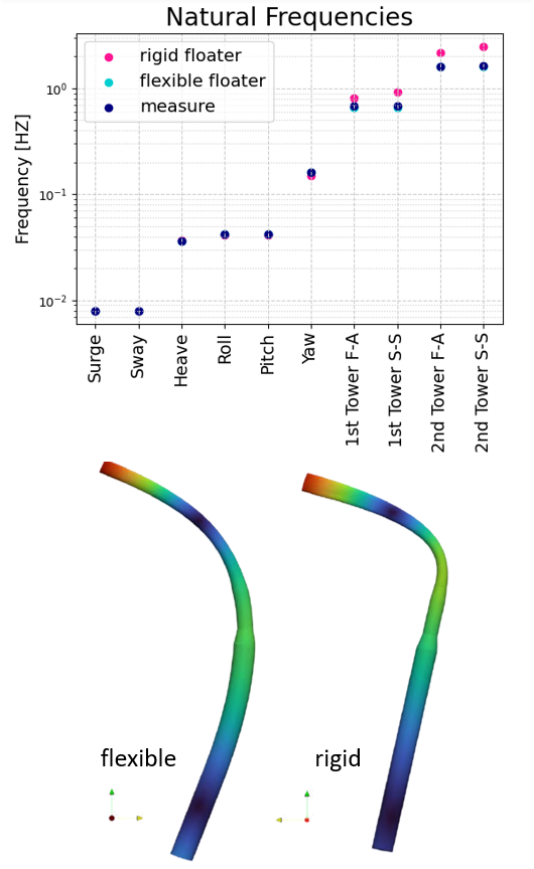

Figure 8. Plot of the measured and simulated natural frequencies of the system (upper figure). Graphical representation of the first fore-aft coupled floater-tower mode (lower image).

3 Results and Discussion

This section is divided into two parts. Following the schema of figure 6 , this section shows the modal sensitivity analysis performed in Homer. In the second part, a spectral analysis of the measured acceleration and the simulation signals is presented.

A 1 hour simulation time was run for each load case in OpenFAST. To avoid the undesired model transient response, the first 300 seconds were eliminated, keeping the equivalent 1 hour simulation when the structure is in its stability position.

3.1 Sensitivity analysis

During this analysis, the effect on the tower modes of the following phenomena and component modeling was evaluated:

- the floater rigidity
- the hydrodynamic added mass
- the flexibility of the blades

This first sensitivity analysis was carried-out in Homer based on the finite element model shown in figure 4. ~~For~~ In the reference case, the ~~rotor nacelle~~ rotor-nacelle assembly (including the blades) and the floater were ~~considered as~~ assumed to be rigid. To approximate the ~~floater structure to the rigid hypothesis in the Homer~~ rigid-floater condition within the HOMER model, the material~~Young modulus was~~ 's Young's modulus was artificially increased from the steel value of $2.1E+11Pa$ to $1E+20Pa$. This unrealistic high modulus was used solely to demonstrate that increasing the floater stiffness in the physically consistent HOMER model causes the system's modal behavior to converge toward the rigid-floater configuration. The adopted value is therefore valid only for the purposes of the present study.

~~Plot of the measured and simulated natural frequencies of the system (upper figure). Graphical representation of the first fore-aft coupled floater-tower mode (lower image).~~

~~On the~~ The upper graph in figure 8 ~~is presented a diagram of~~ presents the natural frequencies of the system. The first ~~6~~ six modes correspond to the ~~6~~ six degrees of freedom (DoFs) of a floating system. ~~Very good agreement has been shown~~ A very good agreement was observed between measured and simulated values, ~~indicating a good~~ confirming the accuracy of the global mass and stiffness ~~description of the system. A~~ representation. The yaw response exhibited the largest deviation, with a maximum error of 7% ~~was estimated when comparing the yaw response. The average error of the 6 degrees of freedom is around~~ while the average error across all six DoFs was approximately 3%. ~~Indeed, the rigid floater showed a minimum~~ As expected, modeling the floater as rigid showed minimal influence on the ~~low frequency~~ low-frequency modes$(1^{st}-6^{th})$.

~~On the contrary, the stiffness of the floater had great influence on the tower modesas is shown on the last four modes in the same image on~~ In contrast, the floater stiffness strongly affected the tower modes, as seen in the higher-order modes in figure 8. ~~A higher error between measurements and simulated tower modes was encountered when considering the floater as rigid, with a higher value up to 33%~~ When the floater was considered rigid, significantly larger discrepancies emerged, with errors reaching up to 37% for the second side-to-side tower mode. Conversely, ~~when the floater is modeled as flexible ,~~ modeling the floater as flexible led to a reduction of the four tower natural frequencies~~drops to better match the measured frequencies~~, resulting in much closer agreement with the measured values. A graphic representation of the first fore-aft coupled floater-tower mode shape is shown on the ~~rigth~~ bottom image of figure 8.

In the second analysis, the ~~effect~~ influence of the hydrodynamic added mass was evaluated. When ~~considering this extra mass , a decreas in the frequencies is exhibited, together with~~ this additional mass was included, a reduction in the natural frequencies was observed, and the average

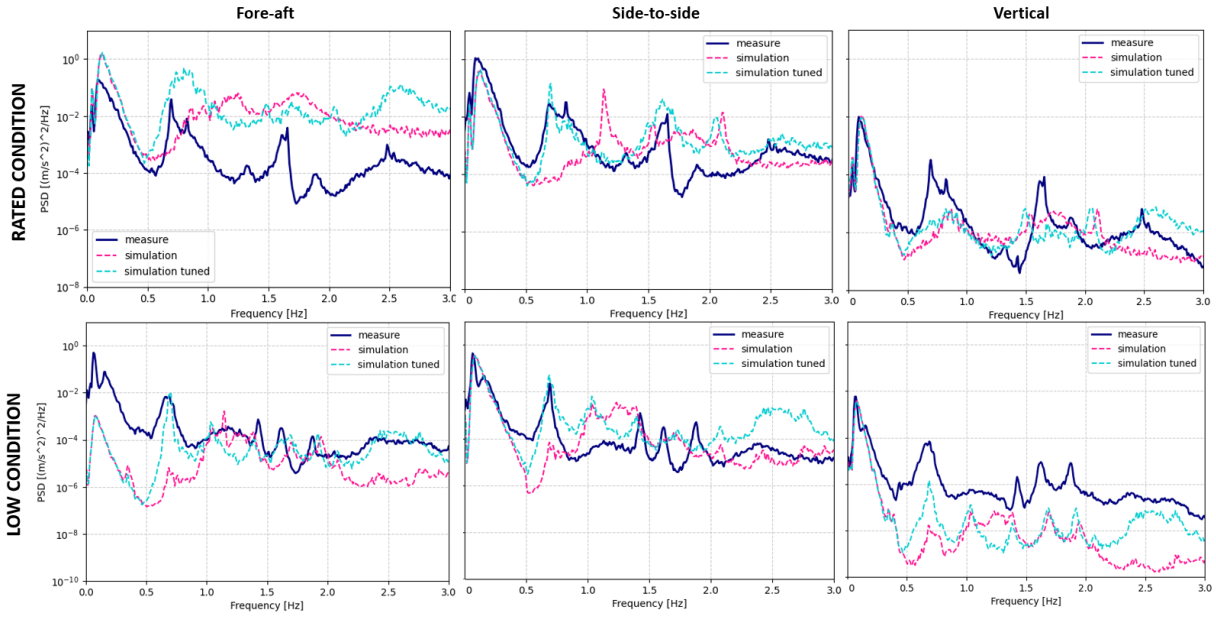

Figure 9. Spectrum of the measured and simulated acceleration of the sensor node 4 in function of the fore-aft, side-to-side and vertical directions. The dark blue line represent the measurement, the pink line is the response of the original model and the light blue line the response of the tuned model.

Table 4. Summary of the estimated tower natural frequencies from the sensitivity analysis.

	S-MORPHO	HOMER			
Tower mode	Measure	Rigid/dry floater	Hydro added mass	Flexible floater	Flexible blades
1st tower SS [Hz]	0.69	1.10	0.96	0.66	0.70
1st tower FA [Hz]	0.69	1.14	0.98	0.66	0.72

error ~~down~~ decreased to 28% (see column 4 in table 4). ~~In the same token, the fifth column shows a more significant decrease of the tower frequencies when the flexibility of the floater is added on top of the additional hydrodynamic mass, with a drop in~~ Subsequently, when floater flexibility was considered in addition to the hydrodynamic added mass, the tower frequencies showed a more pronounced decrease. This adjustment further reduced the average error ~~down to~~ 5% (column 5 in table 4).

In the final ~~analysis, the blades flexibility was considered~~step, blade flexibility was incorporated, while the hub and nacelle were modeled ~~rigidly~~as rigid. A rigid connection was imposed ~~to join the blades root~~ between the blade roots and the hub~~. The~~, and the distributed blade structural properties were ~~obtained~~ taken from the SIMA model developed ~~in (Homb, Hans Rangøyen , 2013)~~by Homb (2013).

~~The blade flexibility has~~ Unlike the floater flexibility, the blade flexibility exhibited an opposite effect ~~in~~ on the tower modes~~. This flexibility has increased by~~, leading to a 7% ~~the last results. It is important to note however, that this increase has diminished the~~ increase in the frequencies compared to the previous results. Nevertheless, this modification improved the overall accuracy, reducing the average error from 5% ~~down~~ to 3% ~~as shown in the~~ (last column in table 4).

~~Summary of the estimated tower natural frequencies from the sensitivity analysis. S-MORPHOHOMER MeasureRigid/dry floaterHydro added massFlexible floaterFlexible blades1st tower SS0.69 1.10 0.96 0.66 0.70 1st tower FA0.69 1.14 0.98 0.66 0.72~~

3.2 Spectral analysis

~~Thus far, it was verified that~~ It was confirmed that modeling the floater as a rigid body significantly affects the ~~rigid body floater modelling has important effects on the~~ tower natural frequencies of the Zefyros FOWT. ~~Therefore, this~~ Consequently, floater flexibility must be ~~taken into account on the time domain~~ accounted for in the time-domain simulation tool. To ~~do~~ achieve this, the ~~so-called~~ tower adjustment factors were ~~modify within~~ modified within the OpenFAST simulator, ~~inside~~ specifically in the ElastoDyn

file. These ~~tower coefficients multiplies~~ coefficients multiply the global tower stiffness for the first and second tower ~~mode in fore -aft~~ modes in both the fore-aft and side-to-side directions. ~~Only the two coefficients of~~ For this study, only the coefficients corresponding to the first tower mode were ~~considered in this study~~adjusted.

~~In order to find the coefficient values , a manual trial and error tuning was done~~ The coefficient values were determined through a manual trial-and-error procedure to fit the measured frequency spectrum shown in figure ~~10. The individual coefficients values that fitted the measured frequencies~~ 9. The resulting adjustment factors were 0.397 ~~and 0.400~~ for the fore-aft ~~and~~ direction and 0.400 for the side-to-side ~~directions respectively~~direction.

To ~~compare the time domain~~ validate the time-domain simulation outputs, ~~4 time domain simulations in OpenFAST were ran. The first two , for a low wind turbine condition with~~ four OpenFAST simulations were conducted: two for the low wind condition (using the original and the adjusted model~~. And 2 more for a rated condition. Hence, the graphs on figure 10 shows the~~) and two for the rated wind condition. Figure 9 presents the acceleration spectrum comparison ~~of~~ for the measured data (dark blue line), ~~of the response of the rigid floater~~ the rigid-floater model (pink dashed line), and the tuned model (light blue dashed line) ~~for low and rated conditions.~~ under both operating conditions. The spectra were computed using Welch's Power Spectral Density method in Python.

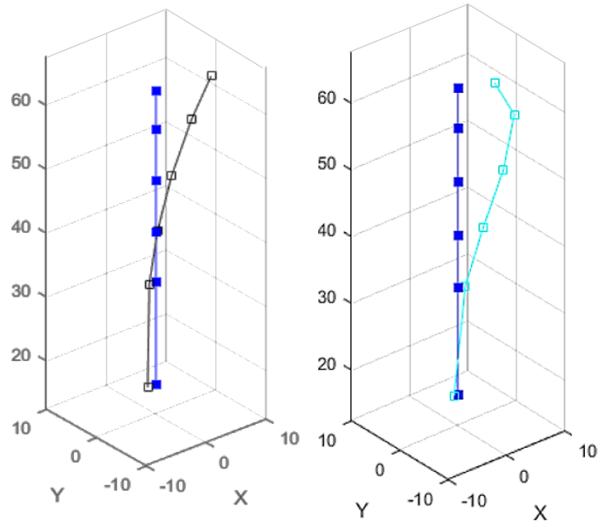

Figure 10. First and second tower mode shapes estimated from OpenFAST acceleration output data by OMA routine. Both images depicts the fore-aft direction..

~~The spectrum was calculated using a Welch's Power Spectral Density on python.~~

The simulated dynamic response in the side-to-side direction (middle graph of figure ~~10) has shown a~~ 9) has showed good agreement within the $0.05 - 3Hz$ frequency range. ~~It is important to note how~~ Notably, the tuned numerical model ~~showed a sweep-off of~~ shifted the original frequency peak from $1.1Hz$ to $0.70Hz$ in both the fore-aft and side-to-side ~~spectrum that corresponds to~~ spectra, corresponding to the first tower frequency. This was ~~validated by applying OMAalgorithm on~~ further validated using the Operational Modal Analysis (OMA) algorithm applied to the acceleration output data, as described in section ~~??. The result~~ 2.1.1, and the resulting modal shape is illustrated ~~on figure 9 that corresponds well to~~ in figure 10, showing excellent agreement with the first tower mode.

~~Taking into account~~ Considering the peak verification, ~~it can be seen that the model fits very well~~ the tuned model accurately captures the first tower mode at $0.69Hz$ and the harmonics due to the rotor rotation, ~~the well known~~ namely the 3P and 6P at $0.83Hz$ and $1.66Hz$ respectively. The model ~~showed lower accuracy in the low frequency content, i.e. between~~ was less accurate in the low-frequency range (0 ~~and~~ to $0.05Hz$~~. This discrepancy may be due to the fact that second order~~), likely because second-order hydrodynamic forces were not ~~considered here~~included in this analysis.

In the fore-aft direction (left images in figure ~~10~~9), the simulation response ~~showed~~ exhibited either higher or lower amplitudes than the measured ~~one along the whole analysed~~ data across the analyzed frequency range. ~~The aforementioned may be due to several facts, as the uncertainty of the~~ This discrepancy may arise from multiple sources, including uncertainties in sensor position and ~~direction,~~ orientation, and the sensor localization within the numerical model relative to the ~~uncertainty on the sensor localization inside the model in function of the~~ tower discretization~~, etc~~.

As a result of the tuning process, ~~and despite~~ although the dynamic response of the model ~~got~~ became closer to the ~~measure~~measured data, the global tower stiffness ~~has been modified, which had impacts on the system response. On top of that, the founded values are~~ was modified, impacting the overall system behavior. Moreover, the obtained values were considerably low, ~~which indicates a significant reduction on the~~ indicating a substantial reduction in tower rigidity. ~~In~~ According to the OpenFAST forum~~it is recommended to use this~~ , these tower stiffness tuners are recommended only for small adjustments, with values not smaller than 0.9. ~~Usually, a stiffness modification in a system can be distinguishes on the low frequency content of a~~ Typically, a modification in system stiffness is most evident in the low-frequency content of the response spectrum. Figure 11 ~~shows~~ illustrates the dynamic response before and after ~~adjusting~~ the tower stiffness ~~. From the figure it can be seen~~ adjustment. It is apparent that the adjustment ~~has effects on low frequency content, for frequencies lower than~~ primarily affects frequencies below $0.01Hz$. ~~Similarly, the~~

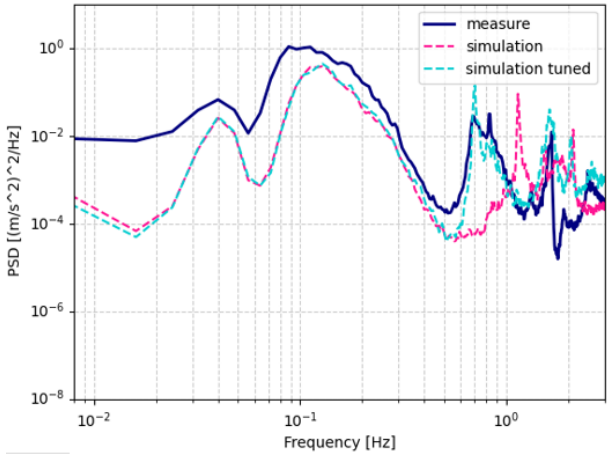

Figure 11. ~~Spectrum~~ Power spectral density of the ~~measured and simulated acceleration of the sensor node 4 in function of the fore-aft,~~ side-to-side ~~and vertical directions. The dark blue line represent the measurement, the pink line is the~~ dynamic response of ~~the original model and the light blue line the response of the tuned model~~sensor number 4. Rated condition.

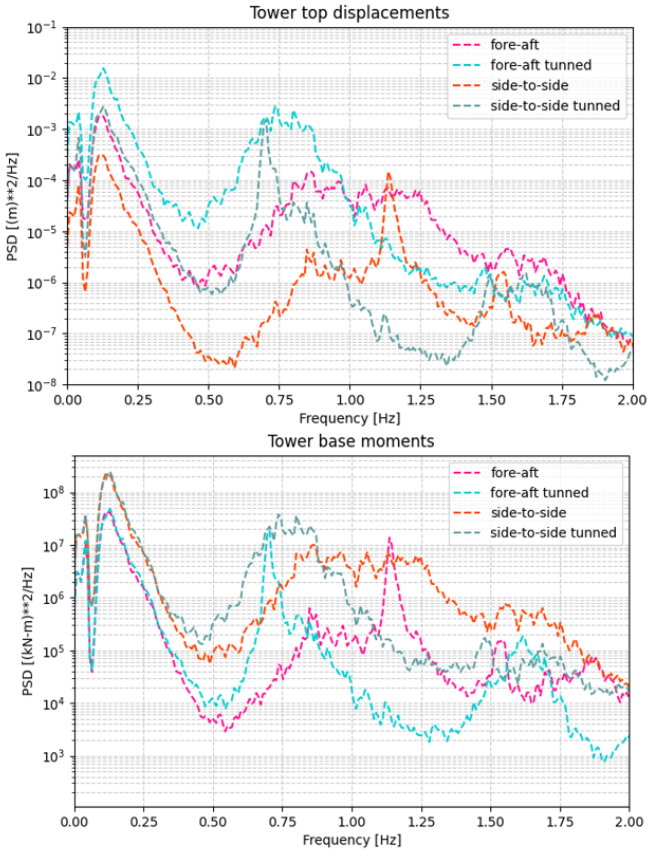

Figure 12. Power spectral density of the ~~side-to-side dynamic response of sensor number 4. Rated condition~~ tower-top displacements (upper image) and the tower-base moment (lower image)

~~displacements and moments of the tower were analyzed to evaluate the influence of the coefficients modification. In the left image on figure 11~~ To further assess the influence of the stiffness modification, tower displacements and moments were analyzed. The upper panel of figure 11 shows the displacements at the ~~displacements of the~~ top of the tower ~~are shown in~~ in both the fore-aft and side-to-side directions. As expected, the amplitudes ~~of the tower displacements increased as the tower stiffness decreased~~increased with the reduction in tower stiffness.

In contrast, the ~~right image in the same figure shows~~ lower panel of figure 11 indicates that the tower-base bending moments ~~on the frequency range of waves excitation~~ within the wave-excitation frequency range $(0 - 0.5Hz)$ ~~was not influenced~~ were not significantly affected by the global stiffness reduction~~of the tower~~.

4 Conclusion

This study investigates the effects ~~the the floater rigid hypothesis~~of the rigid-floater assumption, the hydrodynamic added mass~~and the flexibility of the blades have~~ , and the blade flexibility on the global dynamic response of the 2.3 MW spar-type floating wind turbine Zefyros. ~~A regular and still common practice in the~~ In conventional wind turbine structural ~~analysis is to consider~~ analyses, it is common to model the floater as a rigid body. However, as wind turbines increase in size to capture more energy, this rigid-floater assumption becomes progressively less valid.

~~The tendency of the increasing energy production is directly related to the increase of the wind turbine size . As a result, when the structure increases, the rigid floater hypothesis loses validity. This has been corroborated during this study.~~

It was demonstrated that ~~the effect of the~~ floater flexibility has ~~great influence~~ a substantial impact on the tower modes~~of a 2.3 MW spar-type, with a~~ , with errors reaching up to 37% ~~error in comparison to the measured modes~~when compared to measured modal data.

Hydro-servo-aero-elastic simulation tools can ~~utilize~~ incorporate floater flexibility using a Morison hydrodynamic model~~to account for floater flexibility. When using flow potential hydrodynamic models~~of the floater, ~~we observe that~~ . When employing potential-flow hydrodynamic models, modern simulation tools are ~~progressively integrating new~~ increasingly integrating functionalities to couple distributed hydrodynamic databases with mechanical ~~beam element floatermodels~~beam-element representations of the floater.

When it is not possible to implement a flexible floater in the Hydro-servo-aero-elastic model due to software restrictions, it is generally feasible to modify the tow-

er/floater boundary condition and calibrate the tower's ~~eigen-frequency~~ eigen-frequencies by adding a massless beam with a well-chosen length and stiffness ~~below the tower~~ between the tower and floater. In OpenFAST, one possible solution is adjusting the global tower stiffness factors to properly fit the spectral response to the measured one. We do not recommend using this solution as it modifies the tower's mechanical model itself. However, we implemented it in our case due to limitations of the older OpenFAST version. We observed that this adjustment ~~allowed us to match tower eigen-frequencies in the time domain~~ successfully aligned the tower eigenfrequencies in the time-domain simulations. It ~~has shown to have minimal effects~~ had minimal impact on the low-frequency content of the dynamic response ~~, within the range of (0to ~~ 0.01 Hz~~. Additionally, it increased the ~~) but led to increased~~ tower-top displacements~~as the tower becomes virtually less rigid~~, reflecting the effectively reduced tower rigidity. In contrast, the modification had ~~a small influence on the tower-based~~ only a minor effect on the tower-base bending moments.

~~project.~~

Data availability. Data could be available on demand, in order with the contractual description of DIONYSOS project.

Author contributions. CA: Methodology, Software, Validation, Formal analysis, Investigations, Writing - original draft, Writing - review and editing, Visualization. RR: Methodology, Software, Investigations, Writing - original draft, Writing - review and editing, Project administration. JDL: Methodology, Software, Writing - Original Draft. AH: Methodology, Software,Writing - Original Draft

Competing interests. The authors declare that they have no conflict of interest.

References

~~Homb, Hans Ranøyen.: Fatigue Analysis of Mooring Lines on the Floating Wind Turbine Hywind.2013~~

Abbas, Nikhar J and Zalkind, Daniel S and Pao, Lucy and Wright, Alan: A reference open-source controller for fixed and floating offshore wind turbines. 2022.

~~WWEA: World Market for Wind Power Saw Another Record Year in 2021~~

Aguilera C. and Desbazeille M.: ~~97, 3 Gigawatt of New Capacity Added. 2019.~~ 20240305_DIONYSOS_WP04_Task4.1a_Local SHM digital twin on FOWT floater. 2024.

~~UNITECH: Dynamic cables for offshore wind farms. 2022.~~

Akiba, Takuya and Sano, Shotaro and Yanase, Toshihiko and Ohta, Takeru and Koyama, Masanori : Optuna: A Next-Generation Hyperparameter Optimization Framework https://github.com/optuna/optuna

~~European Commission: Assessment of the final national energy and climate plan of France.2023.~~

Al-Solihat, Mohammed Khair and Nahon, Meyer: Flexible multibody dynamic modeling of a floating wind turbine. 2018.

Allen, C. and Viscelli, A. and Dagher, H. and Goupee, A. and Gaertner, E. and Abbas, N. and Hall, M.D. and Barter, G.: Definition of the UMaine VolturnUS-S Reference Platform Developed for the IEA Wind 15-Megawatt Offshore Reference Wind Turbine: IEA Wind TCP Task 37. 2020.

ANSYS: Online Manual. 2024. https://www.caee.utexas.edu/prof/kallivokas/teaching/ANSYS_examples/ansys56theory.pdf

Berahmand, Kamal and Daneshfar, Fatemeh and Salehi, Elaheh Sadat and Li, Yuefeng and Xu, Yue: Autoencoders and their applications in machine learning: a survey. 2024.

Bir, G. : User's Guide to BModes (Software for Computing Rotating Beam Coupled Modes). 2007. chrome-extension://efaidnbmnnnibpcajpcglclefindmkaj/https://www.nrel.gov/wind/nwtc/assets/pdfs/bmodes.pdf

Borg, Michael and Hansen, Anders Melchior and Bredmose, Henrik: Floating substructure flexibility of large-volume 10MW offshore wind turbine platforms in dynamic calculations. 2016.

Bureau Veritas: Classification and certification of floating offshore wind turbines. 2015.

Cheng, Zhengshun and Wang, Kai and Gao, Zhen and Moan, Torgeir: Comparative study of spar type floating horizontal and vertical axis wind turbines subjected to constant winds. 2015.

Chenyu Luan and Zhen Gao and Torgeir Moan: Development and verification of a time-domain approach for determining forces and moments in structural components of floaters with an application to floating wind turbines. 2017.

C.P.M. Curfs: Dynamic behaviour of floating wind turbines - A comparison of open water and level ice conditions. 2015. https://repository.tudelft.nl/record/uuid:f339482a-8e0d-4827-85af-c8cf05b4260f

de Lauzon Jérome: Coupled eigen-frequency analysis of floating wind turbines. 2024.

DNV-GL: DNV-RP-0286 Coupled analysis of floating wind turbines. 2019.

~~European Commission : Summary of the Commission assessment of the draft National Energy and Climate Plan~~ European Commission : Summary of the Commission assessment of the draft National Energy and Climate Plan 2021-2030. 2019. https://energy.ec.europa.eu/system/files/2019-06/necp_factsheet_fr_final_0.pdf

~~Stadtmann, Florian and Rasheed, Adil and Kvamsdal, Trond and Johannessen, Kjetil André and San, Omer and Kölle, Konstanze and Tande, John Olav and Barstad, Idar and Benhamou, Alexis and Brathaug, Thomas and Christiansen, Tore and Firle, Anouk-Letizia and Fjeldly, Alexander and Frøyd, Lars and Gleim, Alexander and Høiberget, Alexander and Meissner, Catherine and Nygård, Guttorm and Olsen, Jørgen and Paulshus, Håvard and Rasmussen, Tore and Rishoff, Elling and Scibilia, Francesco and Skogås, John Olav: Digital Twins in Wind Energy: Emerging Technologies and Industry-Informed Future Directions.~~

European Commission: Assessment of the final national energy and climate plan of France. 2023. https://commission.europa.eu/

system/files/2023-12/SWD_Assessment_draft_updated_NECP_France_2023.pdf

Joyce Lee, Feng Zhao: Global wind repport

France Energies Marines: Contractual description – Digital Intelligent Operational Network using hYbrid SensOrs / Simulations approach. 2021. 2021.

Redoute, T. : Manuel d'utilisation du systéme neuron. 2020.

Global Wind Energy Council: GLOBAL OFFSHORE WIND REPORT 2023. 2023. https://gwec.net/wp-content/uploads/2023/08/GWEC-Global-Offshore-Wind-Report-2023.pdf

Goodfellow, Ian and Bengio, Yoshua and Courville, Aaron: Deep learning. 2016.

Guignier, Lucie and Courbois, Adrien and Mariani, Riccardo and Choisnet, Thomas: Multibody Modelling of Floating Offshore Wind Turbine Foundation for Global Loads Analysis. 2016.

Hall, Matthew: MoorDyn user's guide. 2015.

Hall, Matthew: Moordyn v2: New capabilities in mooring system components and load cases. 2020.

Haoran Li and Zhen Gao and Erin E. Bachynski-Polić and Yuna Zhao and Stian Fiskvik: Effect of floater flexibility on global dynamic responses of a 15-MW semi-submersible floating wind turbine. 2023.

Hirvoas, A.: Model construction of Zefyros floating offshore wind turbine. 2022.

Hobbacher, AF and others: Recommendations for fatigue design of welded joints and components. 2016.

Skaare, Bjørn and Nielsen, Finn Gunnar and Hanson, Tor David and Yttervik, Rune and Havmøller, Ole and Rekdal, Arne: Analysis of measurements and simulations from the Hywind Demo floating wind turbine. 2015.

Homb, Hans Rangøyen: Fatigue Analysis of Mooring Lines on the Floating Wind Turbine Hywind Demo. 2013.

Goodfellow, Ian and Bengio, Yoshua and Courville, Aaron: Deep learning. 2016.

IRENA: World Energy Transitions Outlook 2023: 1.5°C Pathway. 2023.

Ren21, K: Renewables 2021-Global Status Report: Tech. Rep.

Johnson, Nicholas and Jonkman, Jason and Wright, A and Hayman, Greg and Robertson, A: Verification of floating offshore wind linearization functionality in OpenFAST. 2019.

Jonkman, Jason: TurbSim User's Guide v2.00.00 . 2021. 2016. chrome-extension://efaidnbmnnnibpcajpcglclefindmkaj/https://www.nrel.gov/wind/nwtc/assets/downloads/TurbSim/TurbSim_v2.00.pdf

Jonkman, Jason Mark and Buhl, Marshall L and others: FAST user's guide. 2005.

WindEurope: Wind Energy in Europe: 2021 Statistics and the Outlook for 2022-2026.

Jonkman, Jason M and Robertson, AN and Hayman, Greg J: HydroDyn user's guide and theory manual. 2014.

Joyce Lee, Feng Zhao: Global wind repport 2021. 2021. https://gwec.net/wp-content/uploads/2021/03/GWEC-Global-Wind-Report-2021.pdf

Berahmand, Kamal and Daneshfar, Fatemeh and Salehi, Elaheh Sadat and Li, Yuefeng and Xu, Yue: Autoencoders and their applicationsin machine learning: a survey. 2024.

V. Leroy and E.E. Bachynski-Polić and A. Babarit and P. Ferrant and J.-C. Gilloteaux: A weak-scatterer potential flow theory-based model for the hydroelastic analysis of offshore wind turbine substructures. 2021.

Susan Gourvenec: Floating wind farms: how to make them the future of green electricity. 2020.

Malenica, Š and Tuitman, Johan and Bigot, Fabien and Sireta, Francois-Xavier: Some aspects of 3D linear hydroelastic models of springing. 2008.

Malenica, Š and Derbanne, Quentin and Sireta, Francois-Xavier and Bigot, Fabien and Tiphine, Etienne and De Hauteclocque, Guillaume and Chen, Xiao-Bo: HOMER–Integrated hydro-structure interactions tool for naval and offshore applications. 2013.

Masjedian, M.H. and Keshmiri, Mehdi: A review on operational modal analysis researches: Classification of methods and applications. 2009.

Molin, Bernard: Offshore structure hydrodynamics. 2023.

National Renewable Energy Laboratory (NREL): OpenFast. 2024. https://github.com/OpenFAST

Nava, V. and Ruiz-Minguela, P. and Perez-Moran, G. and Rodriguez Arias, R. and Lopez Mendia, J. and Villate-Martinez, J.-L.: Installation, Operation and Maintenance of Offshore Renewables. 2019.

Oliveira, Gustavo and Magalhães, Filipe and Cunha , Álvaro and Caetano, Elsa : Continuous dynamic monitoring of an onshore wind turbine. 2018.

Pastor, Miroslav and Binda, Michal and Harčarik, Tomáš : Modal Assurance Criterion. 2012.

Redoute, T.: S-MORPHO system user manual. 2020.

Ren21, K: Renewables 2021-Global Status Report: Tech. Rep.. 2021.

Simulation Optimisation Parameters Package (Version 1.0) [Software] https://gitlab.france-energies-marines.org/Romain/simuoptuna

Schlechtingen, Meik and Santos, Ilmar Ferreira and Achiche, Sofiane: Wind turbine condition monitoring based on SCADA data using normal behavior models. Part 1: System description. 2013.

Schlechtingen, Meik and Santos, Ilmar Ferreira: Wind turbine condition monitoring based on SCADA data using normal behavior models. Part 2: Application examples. 2014.

Aguilera C. and Desbazeille M.: 20240305 DIONYSOS WP04 Task4.1a Local SHM digital twin on FOWT floater

SERCEL: S-MORPHO system – Specifications of calculation algoritms. 2024.

IRENA: World Energy Transitions Outlook 2023: 1.5°C Pathway. 2023.

Sjur Neuenkirchen Godø: Dynamic Response of Floating Wind Turbines. 2013.

WindEurope: Floatting Offshore Wind. 2020.

Skaare, Bjørn and Nielsen, Finn and Hanson, Tor and Yttervik, Rune and Havmøller, Ole and Rekdal, Arne: Analysis of measurements and simulations from the Hywind Demo floating wind turbine: Dynamic analysis of the Hywind Demo floating wind turbine. 2014.

Skaare, Bjørn and Hanson, Tor and Nielsen, Finn and Yttervik, Rune and Hansen, Anders and Thomsen, Kenneth and Larsen,

Torben and Skaare@hydro, Bjorn and No, and David, Tor and No, Finn and Gunnar, and Com, Rune and No, Anders and Melchio: Integrated dynamic analysis of floating offshore wind turbines. 2007.

Sjur Neuenkirchen Godø: Dynamic Response of Floating Wind Turbines. 2013.

Skaare, Bjørn and Nielsen, Finn and Hanson, Tor and Yttervik, Rune and Havmøller, Ole and Rekdal, Arne: Analysis of measurements and simulations from the Hywind Demo floating wind turbine: Dynamic analysis of the Hywind Demo floating wind turbine. 2014.

Skaare, Bjørn and Nielsen, Finn and Hanson, T.D. and Yttervik, Rune and Havmøller, Ole and Rekdal, A.: Analysis of measurements and simulations from the Hywind Demo floating wind turbine. 2015.

C.P.M. Curfs: Dynamic behaviour of floating wind turbines - A comparison of open water and level ice conditions. 2015.

Cheng, Zhengshun and Wang, Kai and Gao, Zhen and Moan, Torgeir: Comparative study of spar type floating horizontal and vertical axis wind turbines subjected to constant winds. 2015.

Zhang, Lixian and Shi, Wei and Karimirad, Madjid and Michailides, Constantine and Jiang, Zhiyu: Second-order hydrodynamic effects on the response of three semisubmersible floating offshore wind turbines. 2020.

Haoran Li and Zhen Gao and Erin E. Bachynski-Polić and Yuna Zhao and Stian Fiskvik: Effect of floater flexibility on global dynamic responses of a 15-MW semi-submersible floating wind turbine.

Stadtmann, Florian and Rasheed, Adil and Kvamsdal, Trond and Johannessen, Kjetil André and San, Omer and Kölle, Konstanze and Tande, John Olav and Barstad, Idar and Benhamou, Alexis and Brathaug, Thomas and Christiansen, Tore and Firle, Anouk-Letizia and Fjeldly, Alexander and Frøyd, Lars and Gleim, Alexander and Høiberget, Alexander and Meissner, Catherine and Nygård, Guttorm and Olsen, Jørgen and Paulshus, Håvard and Rasmussen, Tore and Rishoff, Elling and Scibilia, Francesco and Skogås, John Olav: Digital Twins in Wind Energy: Emerging Technologies and Industry-Informed Future Directions. 2023.

Allen, C. and Viscelli, A. and Dagher, H. and Goupee, A. and Gaertner, E. and Abbas, N. and Hall, M.D. and Barter, G.: Definition of the UMaine VolturnUS-S Reference Platform Developed for the IEA Wind 15-Megawatt Offshore Reference Wind Turbine: IEA Wind TCP Task 37. 2020.

Loup

Suja-Thauvinand ,Loup and Krokstad, Jørgen R. Krokstad and and Bachynski, Erin E. Bachynski and Erik-Jan: Experimental results of a multimode monopile offshore wind turbine support structure subjected to steep and breaking irregular waves. 2017.

Zhixin Zhao and Wenhua Wang and Wei Shi and Shengwenjun Qi and Xin Li: Effect of floating substructure flexibility of large-volume 10 MW offshore wind turbine semi-submersible platforms on dynamic response. 2022.

Susan Gourvenec: Floating wind farms: how to make them the future of green electricity. 2020.

Mohammed Khair Al-Solihat and Meyer Nahon: Flexible multibody dynamic modeling of a floating wind turbine. 2018.

Thomsen, Jonas Bjerg and Bergua, Roger and Jonkman, Jason and Robertson, Amy and Mendoza, Nicole and Brown, Cameron and Galinos, Christos and Stiesdal, Henrik: Modeling the TetraSpar Floating Offshore Wind Turbine Foundation as a Flexible Structure in OrcaFlex and OpenFAST. 2012.

Xiaoming Ran and Vincent Leroy and Erin E. Bachynski-Polić: Hydroelastic response of a flexible spar floating wind turbine: Numerical modelling and validation. 2023.

France Energies Marines: Contractual description – Digital Intelligent Operational Network using hYbrid SensOrs / Simulations approach. 2021.

Hirvoas, A.: Model construction of Zefyros floating offshore wind turbine

UNITECH: Dynamic cables for offshore wind farms. 2022. https://www.techtransfer.no/en/renewable-energy/unitech/

Redoute, T.: S-MORPHO system user manual. 2020.

Gustavo Oliveira and Filipe Magalhães and Álvaro Cunha and Elsa Caetano: Continuous dynamic monitoring of an onshore wind turbine. 2018.

van Vondelen, A. A. W. and Navalkar, S. T. and Iliopoulos, A. and van der Hoek, D. C. and van Wingerden, J.-W.: Damping identification of offshore wind turbines using operational modal analysis: a review. 2022.

Masjedian, M.H. and Keshmiri, Mehdi: A review on operational modal analysis researches: Classification of methods and applications. 2009.

Miroslav Pastor and Michal Binda and Tomáš Harčarik: Modal Assurance Criterion. 2012.

National Renewable Energy Laboratory (NREL): OpenFast. 2024.

Malenica, Šand Tuitman, Johan and Bigot, Fabien and Sireta, Francois-Xavier: Some aspects of 3D linear hydroelastic models of springing. 2008.

Malenica, Šand Derbanne, Quentin and Sireta, Francois-Xavier and Bigot, Fabien and Tiphine, Etienne and De Hauteclocque, Guillaume and Chen, Xiao-Bo: HOMER–Integrated hydro-structure interactions tool for naval and offshore applications. 2013.

SERCEL: SERCEL, title = S-MORPHO system – Specifications of calculation algoritms. 2024.

ANSYS: Online Manual. 2024.

B. J. Jonkman: TurbSim User's Guide v2.00.00 . 2016.

Gunjit S. Bir : User's Guide to BModes (Software for Computing Rotating Beam Coupled Modes). 2007.

Jonkman, Jason Mark and Buhl, Marshall L and others: FAST user's guide. 2005.

Hall, Matthew: MoorDyn user's guide. 2015.

Abbas, Nikhar J and Zalkind, Daniel S and Pao, Lucy and Wright, Alan: A reference open-source controller for fixed and floating offshore wind turbines. 2022.

Hall, Matthew: Moordyn v2: New capabilities in mooring system components and load cases.

WindEurope: Floatting Offshore Wind. 2020.

Jonkman, Jason M and Robertson, AN and Hayman, Greg J: HydroDyn user's guide and theory manual. 2014.

WindEurope: Wind Energy in Europe: 2021 Statistics and the Outlook for 2022-2026. 2021. https://windeurope.org/intelligence-platform/product/wind-energy-in-europe-2021-statistics-and-the-outlook-for-2022-2026/

Molin,Bernard: Offshore structure hydrodynamics. 2023.
DNV-GL: DNV-RP-0286 Coupled analysis of floating wind turbines
WWEA: World Market for Wind Power Saw Another Record Year in 2021: 97,3 Gigawatt of New Capacity Added. 2019. https://wwindea.org/world-market-for-wind-power-saw-another-record-year-in-2021-973-gigawatt-of-newcapacity-added/
Veritas, Bureau: Classification and certification of floating offshore wind turbines. 2015.
Homb, Hans Rønøyen: Fatigue Analysis of Mooring Lines on the Floating Wind Turbine Hywind Demo. 2013.
Johnson, Nicholas and Jonkman, Jason and Wright, A and Hayman, Greg and Robertson, A: Verification of floating offshore wind linearization functionality in OpenFAST. 2019.
Thomsen, Jonas Bjerg and Bergua, Roger and Jonkman, Jason and Robertson, Amy and Mendoza, Nicole and Brown, Cameron and Galinos, Christos and Stiesdal, Henrik: Modeling the TetraSpar Floating Offshore Wind Turbine Foundation as a Flexible Structure in OrcaFlex and OpenFAST. 2012.
Xiaoming Ran and Vincent Leroy and Erin E. Bachynski-Polić: Hydroelastic response of a flexible spar floating wind turbine: Numerical modelling and validation. 2023.
de Lauzon Jérome: Coupled eigen-frequency analysis of floating wind turbines. 2024.
Xu, Kun and Zhang, Min and Shao, Yanlin and Gao, Zhen and Moan, Torgeir : Effect of wave nonlinearity on fatigue damage and extreme responses of a semi-submersible floating wind turbine. 2019.
Borg, Michael and Hansen, Anders Melchior and Bredmose, Henrik: Floating substructure flexibility of large-volume 10MW offshore wind turbine platforms in dynamic calculations. 2016.
Chenyu Luan and Zhen Gaoand Torgeir Moan: Development and verification of a time-domain approach for determining forces and moments in structural components of floaters with an application to floating wind
Zhang, Lixian and Shi, Wei and Karimirad, Madjid and Michailides, Constantine and Jiang, Zhiyu: Second-order hydrodynamic effects on the response of three semisubmersible floating offshore wind turbines. 2017. 2020.
Guignier, Lucie and Courbois, Adrien and Mariani, Riccardo and Choisnet, Thomas: Multibody Modelling of Floating Offshore Wind Turbine Foundation for Global Loads Analysis. 2016.
V. Leroy and E.E. Bachynski-Polić and A. Babarit and P. Ferrant and J.-C. Gilloteaux: A weak-scatterer potential flow theory-based model for the hydroelastic analysis of offshore wind turbine substructures. 2021.
Kun Xu and Min Zhang and Yanlin Shao and Zhen Gao and Torgeir Moan
Zhixin Zhao and Wenhua Wang and Wei Shi and Shengwenjun Qi and Xin Li: Effect of wave nonlinearity on fatigue damage and extreme responses of a semi-submersible floating wind turbine. 2019. floating substructure flexibility of large-volume 10 MW offshore wind turbine semi-submersible platforms on dynamic response. 2022.